Integrating Offshore Hydrodynamic Model Output with Onshore Observations to Improve Correctors to Hydrographic Survey Soundings

Lijuan Huang, David Wolcott, and Louis Licate
NOAA/NOS/Center for Operational Oceanographic Products and Services (CO-OPS) 1305 East-West Highway, Silver Spring, MD 20910-3218 (301)-713-2890

Jindong Wang, Barry Gallagher, Edward Myers, and Lei Shi
NOAA/NOS/OCS/Coast Survey Development Laboratory (CSDL) 1315 East-West Highway, Silver Spring, MD 20910-3218

Abstract
NOAA develops tide correctors for reducing hydrographic survey soundings to Chart Datum by using the Tidal Constituent and Residual Interpolation (TCARI) software to interpolate harmonic constants (HCs), tidal datum elevation relationships, and water level residuals from water level gauge observations. The accuracy of the interpolation relies heavily on the spatial distribution of historical and operating water level gauges, which are generally located along the shoreline. Measurements from offshore and mid-estuary data points are typically very sparse. In an effort to develop a higher quality representation of tidal propagation, especially in offshore and tidally complex areas, the integration of the offshore HCs from high resolution tide models into the TCARI interpolation was explored. This paper first describes the process by which the tidal model output is examined and then discusses the incorporation of the model output into the TCARI interpolation of tidal features in the Bering Sea. Options for selecting model points to be input into TCARI were evaluated through a series of sensitivity tests. These tests evaluated how many model points were needed, as well as where they were needed, to resolve tidal features such as amphidromes in the open ocean while still allowing for a smooth transition of the interpolation to nearshore observations. Results indicate that integrating tide model output with observations improves the accuracy of TCARI grids for use in constructing water level reducers for hydrographic surveys. Further testing and validation in other regions is needed to refine the methods and develop a standard operating procedure for its implementation.

Introduction
NOAA's Center for Operational Oceanographic Products and Services (CO-OPS) supports NOAA's nautical charting mission by providing vertical control and water level reductions to the National Ocean Service's (NOS) Office of Coast Survey (OCS) and National Geodetic Survey (NGS). The foundation of accurate vertical control and water level reductions is a network of continuously operating water level stations managed by CO-OPS, called the National Water Level Observation Network (NWLON). NWLON stations provide long-term observations, tidal datum references and harmonic constants (HCs) for tidal reduction scheme development. This paper focuses on the implications for one tide reduction method, Tidal Constituent and Residual Interpolation (TCARI) (Hess 2002 and 2003).

TCARI spatially interpolates the amplitude and phase for major tidal harmonic constituents, tidal datum elevation differences, and water level residuals (i.e., the non-tidal component or the difference between the astronomically predicted tide and the observed water level) over an

unstructured triangular grid by solving Laplace's equation constrained by boundary conditions (Hess 2002 and 2003). Once the TCARI interpolation field is generated for a grid, the water level data series can be derived at any given point within the grid. As the interpolation does not incorporate any tidal physics, the accuracy of TCARI largely relies on the spatial distribution and availability of historical and observed data. In estuaries or large embayments bounded by a substantial number of stations and having relatively simple tidal hydrodynamics, TCARI performs well as tidal features can be readily captured by observations along the shoreline. In offshore areas, extrapolation using TCARI can result in large uncertainties since TCARI directly extrapolates the HCs and tidal datums from the coast to the open ocean. Similarly, TCARI cannot effectively interpolate through semi-amphidromic points or amphidromic points that often occur near the shore in tidally complex areas due to a lack of sufficient spatial resolution of observations. In an effort to develop a higher quality representation of tidal propagation, especially in offshore and tidally complex areas, the integration of the offshore HCs from high resolution tide models into the TCARI interpolation was explored.

The Bering Sea was chosen as a case study as it is becoming a priority area for NOAA to update nautical chart products and it presents many challenges for developing tide reducers using tidal zoning and TCARI. The challenges can be broken into three components 1) a complex tidal regime 2) variable meteorological influence and 3) limited coastal observations in the interpolation domain. The challenges of a complex tidal regime and limited coastal observations can be addressed by integrating the offshore HCs from high resolution tidal models into the TCARI interpolation.

The Bering Sea has a complex tidal regime with several diurnal and semidiurnal amphidromes (Liu and Leendersts 1982, Mofjeld 1986, Pearson et al.1981, Kowalik 1999 and Foreman 2006). An amphidromic point is a point of zero vertical displacement of one harmonic constituent of the tide. The amplitude of that harmonic constituent increases with distance away from this point and the phase of the constituent changes continuously around the central point. The "bullseyes" in Figure 1 show the locations of suspected amphidromic points. In addition to amphidromic points, tidal ranges vary from several centimeters in the Bering Strait to several meters in Bristol Bay. The type of tide transitions between mixed semidiurnal, mixed diurnal and diurnal tides. The shallow water coupled with highly variable meteorological influences in the Bering Sea also complicates the interpolation and results in higher uncertainty.

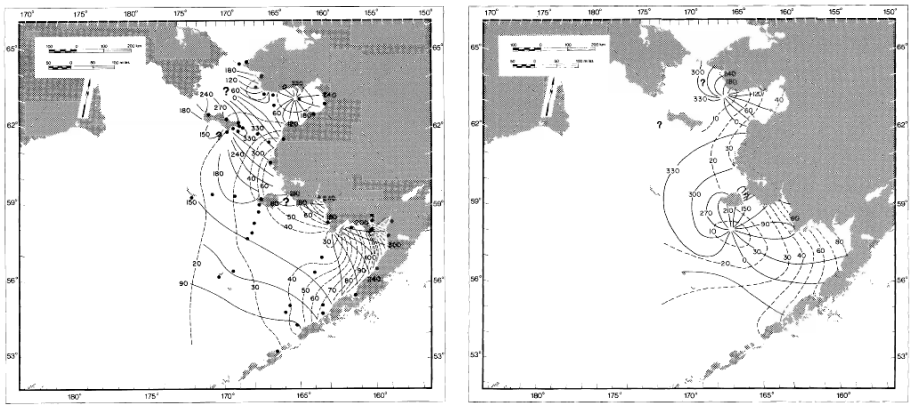

Figure 1. The amplitude and phase contours for M2 (left) and K1 (right) constituents (Pearson et al., 1981)

The complex tidal regime is difficult to capture due to the limited number of available tidal observations along the Bering Sea Coast in Alaska. Currently, there are only four NWLON water level stations along the Bering Sea coastline: Unalaska, Village Cove, Port Moller, and Nome (Figure 2). Twenty seven (27) short-term stations (one-to three months of continuous observations) have been installed in this region since 2003 for different purposes to support either hydrographic surveys or the NOAA Vertical Datum transformation (VDatum) Program. The geographic distribution of NWLON and recent short-term installations is very sparse along the Bering Sea shoreline (Figure 2). Logistical challenges, such as the remote nature of the Bering Sea shoreline, the lack of infrastructure, and seasonal ice coverage, cause operational difficulties in installing and maintaining water level gauges and have resulted in limited coastal observations. Almost all observations are located along the eastern Bering Sea shore. There remains a lack of HCs or tidal observations in the western extent of the TCARI domain.

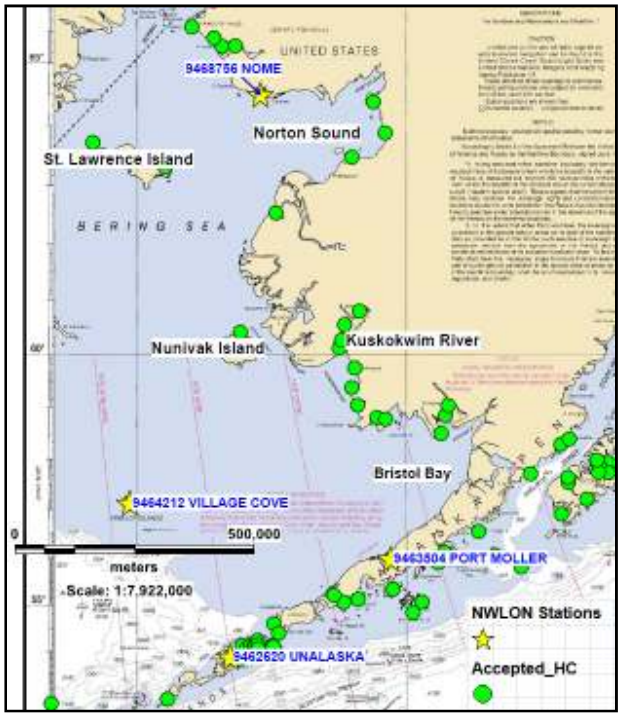

Figure 2. NWLON stations and historical stations with accepted HCs. The blue labels are the stations names and the black labels are geographic names.

A regional tide model developed by Foreman et al. (2006) was used to test the general concept and operational feasibility of the blended method. This tide model assimilated satellite altimetry data and has high accuracy in the offshore area. The modeled HCs were first evaluated by comparison with the CO-OPS published HCs at coastal stations before incorporating them into the TCARI interpolation.

This paper is organized as follows: Section 2 presents the method for evaluating model output and two different methods for selecting model points to be input into TCARI interpolation. Section 3 summarizes the model evaluation results and the comparison of 6 different scenarios (observed only, model only and 4 blended scenarios) of integrating model output with

observations to improve the TCARI interpolation. Section 4 includes a discussion of potential operational implications and future work.

2. Method

A. Model Evaluation

The Foreman tidal model was evaluated by comparing the amplitudes and phases of the tidal constituent output with the published amplitudes and phases of the constituents from tide stations located along the model's land boundary. For this evaluation the principle semidiurnal constituent, M2, and principle diurnal constituent, K1, were used for comparison.

A root mean squared error (RMSE) was computed for each constituent at each location using Equation 1, which combines the amplitude and phase errors. In Equation 1, A_e is the RMSE, A_m is the amplitude of the constituent from the model, A_o is the observed amplitude of the constituent , h_m is the phase of the model constituent, and h_o is the observed phase of the constituent.

$$A_e = \left(\frac{1}{2\pi}\int_0^{2\pi} (A_m \cos(\phi - h_m) - A_o \cos(\phi - h_o))^2 \, d\phi\right)^{\frac{1}{2}}$$

$$= \left(\frac{A_m^{\,2}}{2} + \frac{A_o^{\,2}}{2} - A_m A_o \cos(h_m - h_o)\right)^{\frac{1}{2}} \qquad (1)$$

$$\text{Relative RMSE (\%)} = \frac{A_e}{A_o} \qquad (2)$$

The relative RMSE (%) was determined by dividing the RMSE by the observed amplitude of the constituent (Equation 2) which provides a measure of the relative performance of the model for each constituent. However, it should be noted that for constituents with minimal amplitude, any discrepancy will result in a large relative RMSE. Thus the model evaluation requires an examination of both the absolute RMSE value as well as the relative RMSE.

B. Model Output Integration

After evaluating the model output, a method of integrating tide model output with onshore CO-OPS observations for TCARI interpolation was examined. A number of offshore model output points were selected to be combined with the onshore stations for interpolation, so that the interpolated HCs in the offshore regions were mainly controlled by the model results and the interpolated HCs in the nearshore regions were mainly controlled by the onshore observations. Two ways of selecting model points were investigated. One method involved the manual selection of model points based on spatial distribution of modeled amphidromes. The other method used a program that automatically selects evenly distributed model points throughout the TCARI domain.

The amphidrome-based selection method used the co-amplitude and co-phase contours of six principal tidal constituents (M2, S2, N2, K1, O1, and P1) from the tide model results (Foreman et al., 2006) to select model points around suspected amphidromes. For each constituent, the model point closest to the local minimum amplitude was chosen. Additional model points surrounding the local minimum were selected in order to ensure that the surrounding phase changes were taken into account. Additionally, offshore points were arbitrarily selected to fill the domain. As a result, 129 model grid points (shown in Figure 3, bottom right) were selected to be combined with onshore CO-OPS tide stations in the domain of the Bering Sea of western Alaska.

For the evenly-distributed selection method, a program was designed to automatically select evenly distributed model points in the domain. This program allows the users to define three main parameters: the spatial density, the searching buffer, and the distance from observations. The spatial density parameter controls the rectangular grid size of selected model points. The searching buffer defines the radius of searching model points around the rectangular grid points. The distance from observations is used to eliminate the selected model points that are close to the observations. In this study, three evenly distributed scenarios are evaluated: 1) 100 km spatial density, 30 km distance away from observed stations (G100 D30), 2) 80 km spatial density, 50 km distance away from observed stations (G80 D50), and 3) 50 km spatial density, 25 km distance away from observed stations (G50 D25). All of the 3 evenly distribution scenarios have a 20 km searching buffer distance (Figure 3 and Table 1).

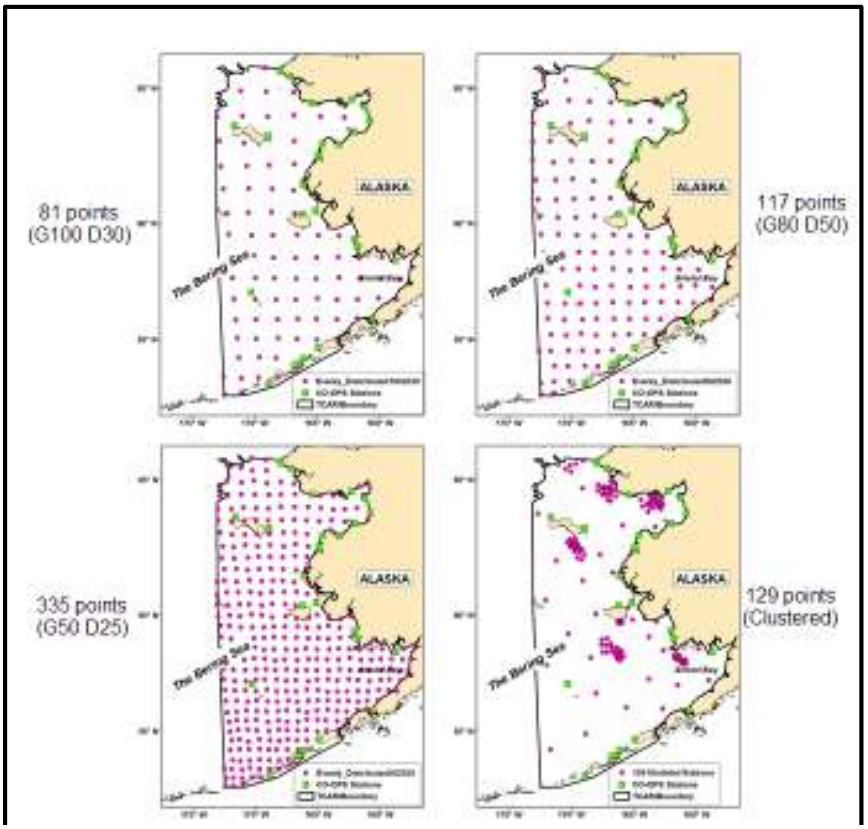

Figure 3. Each of the four "blended" scenarios combining CO-OPS stations with different model output distributions. The grid size (G) and the distance away from stations (D) are shown to the left or right of each scenario.

Table 1: Details of four model point distributions used in the TCARI interpolation sensitivity test. All evenly distributed methods use a 20km searching buffer distance.

Number of Points	Grid Size (km)	Distance from Observed (km)	Method
81	100	30	Even
117	80	50	Even
335	50	25	Even
129	n/a	n/a	Clustered

The selected model grid points from either of the two methods are then combined with CO-OPS tide stations for input into the TCARI interpolation scheme. A triangular mesh with 69,369 nodes, with the resolution varying from a few meters to 30 km, was developed for TCARI interpolation. This type of mesh has much higher resolution around the coast than in the offshore regions. Thus, TCARI should be able to capture the nearshore tidal variations very well given the appropriate distribution and number of interpolation points. The HCs at the onshore tide stations and the selected model points are then interpolated onto the triangular mesh.

3. Results

A. Model Evaluation Results

Figure 4 below shows the relative RMSE values at each of the 18 stations used in the comparison. There is significant variability in the relative RMSEs for both K1 and M2 constituents. The relative RMSE values for the M2 constituent range from 2.4% - 180% and from 3.8% - 90% for the K1 constituent. Given the discrepancies, accurate tide reductions cannot rely only on the hydrodynamic tide model.

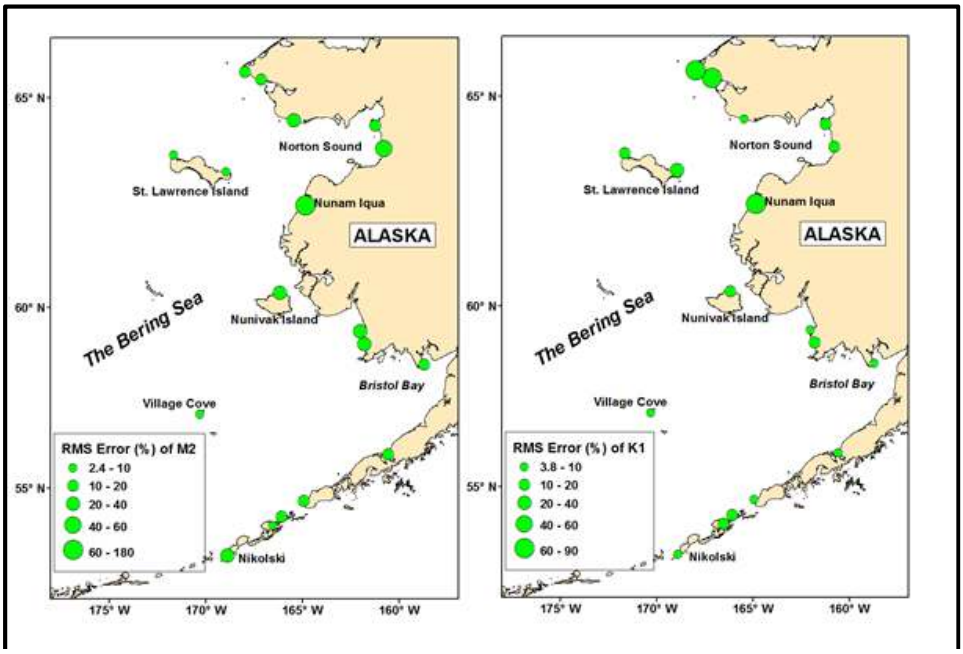

Figure 4. Relative RMSE of M2 and K1 at each of the CO-OPS historical locations

Both the diurnal and semidiurnal constituent differences between the tidal model and observations are highest near the coastal station Nunam Iqua. The model overestimates the amplitudes of both the K1 and M2 constituents at this point and shows a significant phase difference. The model shows an M2 amplitude of 0.58m and phase of 357º while the observations indicate an amplitude of 0.20m and a phase of 54º. Similarly the model shows a K1 amplitude of 0.35m and a phase of 348º while the observations indicate an amplitude of 0.19m and a phase of 24º. These differences are supported by a set of unpublished, historical data near Nunam Iqua. The data collected in the summers of 1982 and 1983 from a station located at Kwikluak also show significant differences in amplitude and phase between the model points and coastal observations. Both Nunam Iqua and Kwikluak are located at the mouth of the Yukon River, roughly 6NM from each other, and have similar amplitudes and phases. Figure 5 below shows the relative locations of Nunam Iqua and Kwikluak in the Yukon Delta and Table 2 shows the values of the modeled and observed differences for K1 and M2.

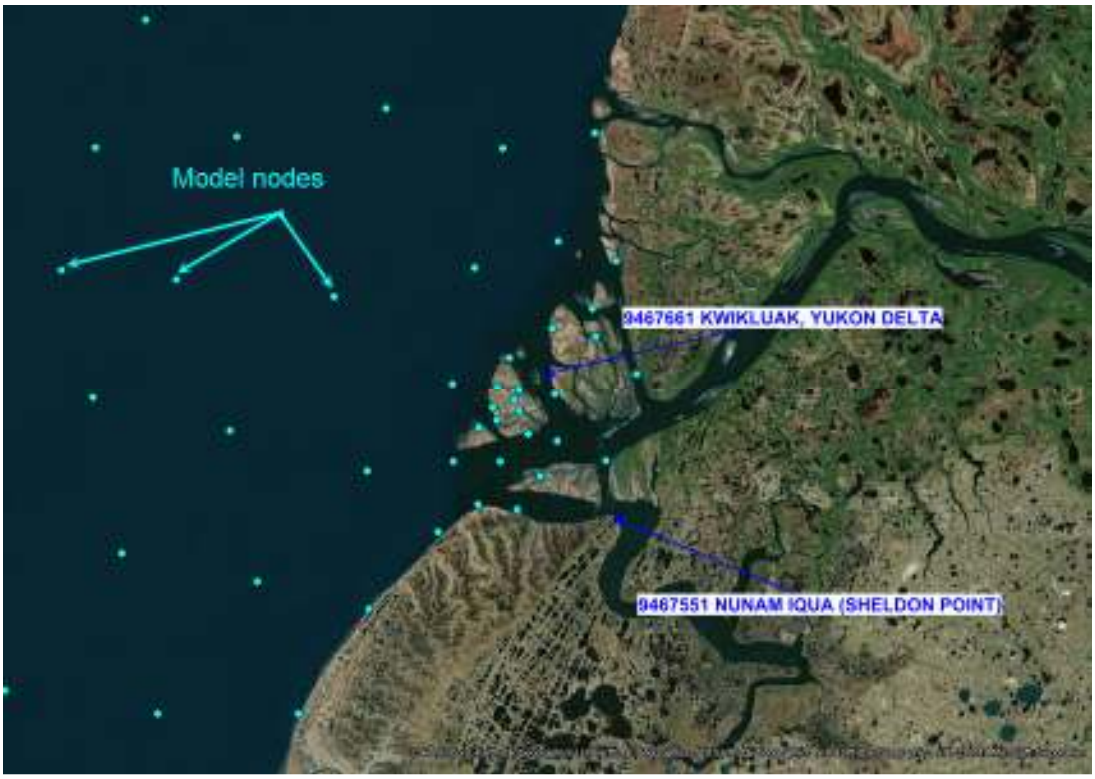

Figure 5. Locations of Nunam Iqua and Kwikluak in the Yukon Delta and the tide model nodes

Table 2. Comparison of the modeled and observed K1 and M2 at Nunam Iqua and Kwikluak

Data Type		9467551 Nunam Iqua		9467661 Kwikluak	
		Amp (m)	Phase (degree)	Amp (m)	Phase (degree)
M2	Obs	0.20	54.1	0.26	44.0
	Foreman	0.58	357.4	0.57	358.4
K1	Obs	0.19	23.9	0.23	14.6
	Foreman	0.35	348.3	0.35	348.9

Plots of the M2 and K1 constituents for Nunam Iqua are shown in Figure 6 and similar plots for Kwikluak are shown in Figure 7. In both figures the constituent information derived from observations is shown in blue and the model output is shown in red.

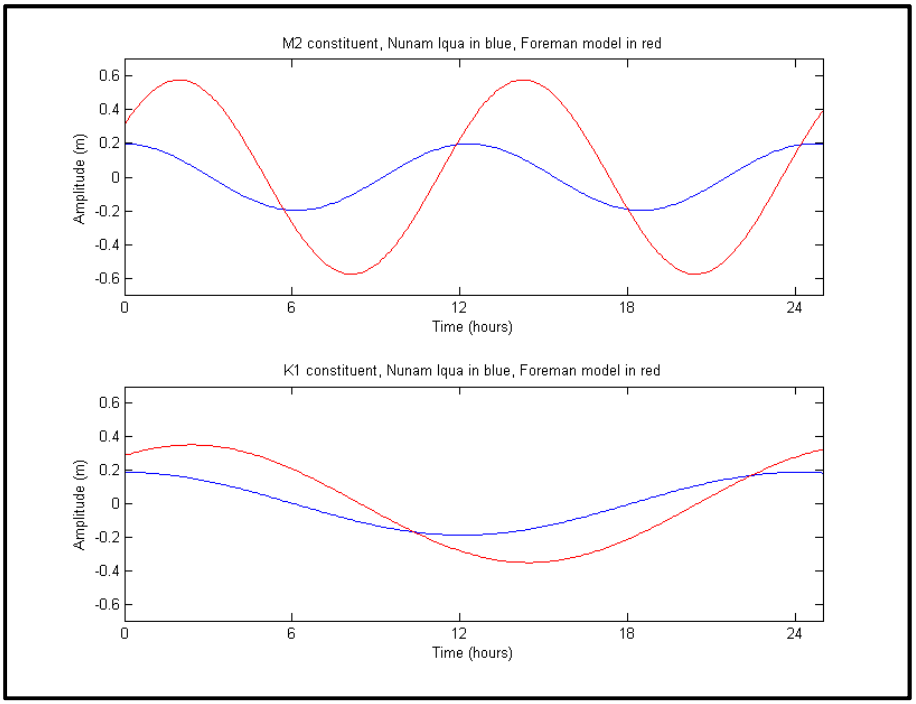

Figure 6. Differences in the harmonic constituents, M2 and K1, at Nunam Iqua

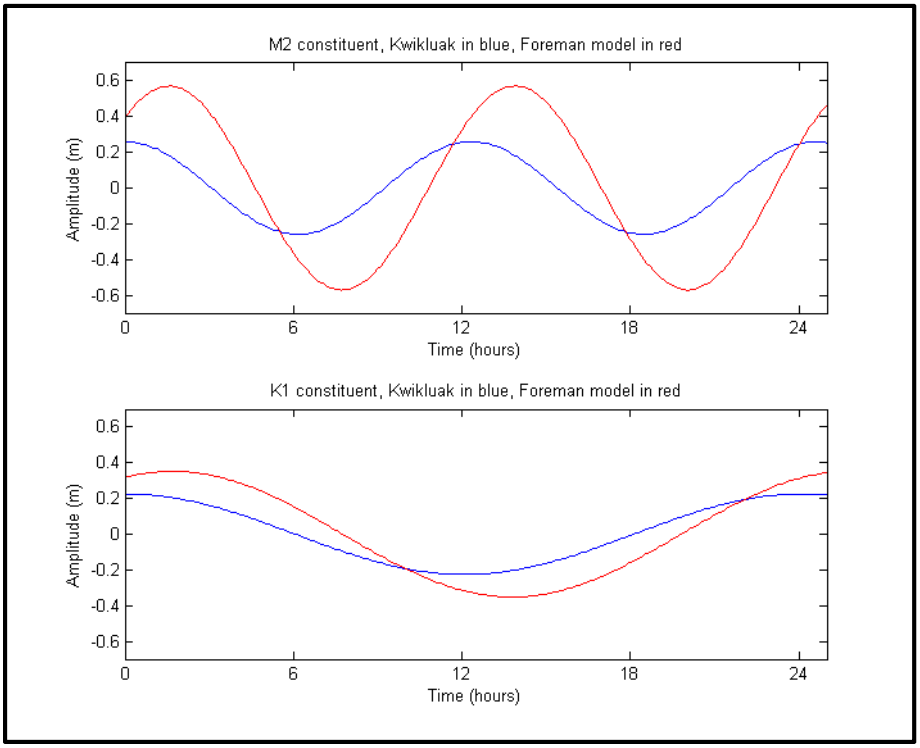

Figure 7. Differences in the harmonic constituents, M2 and K1, at Kwikluak

B. Model Integration Results

A total of six scenarios were used for comparison with a number of datasets collected offshore during the 1980s. The scenarios include the four "blended" TCARI grids shown in Figure 3, the TCARI grid using only data from CO-OPS stations, and the tide model output directly. All six scenarios were compared against data collected during two Pacific Marine Environmental Lab (PMEL) studies in the Bering Sea (Pearson et al., 1981 and Mofjeld, 1986). There were a number of pressure gauges deployed from the tip of the Seward Peninsula south to the end of the Alaskan Peninsula and the data from 24 gauges were used for this comparison. Figure 8 shows the distribution of the pressure gauge locations (red triangle) and the historical CO-OPS stations (green square).

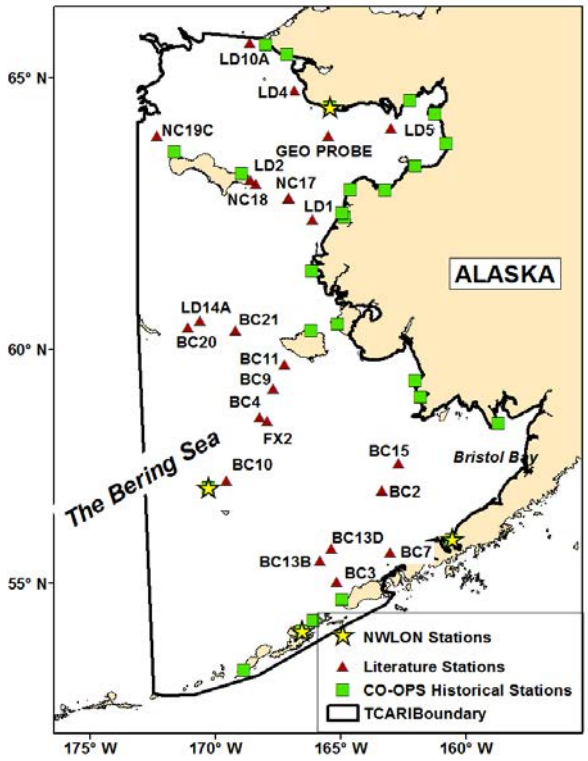

Figure 8. PMEL stations (red triangles) with CO-OPS historical stations (green squares), CO-OPS NWLON stations (yellow stars), and the TCARI grid boundary.

The HCs from each of the six scenarios were compared with the HCs derived from the PMEL observations. The relative RMSE value was computed for M2 and K1 at each location for each of the six scenarios using Equation 1. The results for the M2 and K1 constituent comparisons are shown in Figures 9 and 10. The four blended TCARI solutions, incorporating four model output distributions and the observed data are labeled as "T-mod[number of model points]" while the TCARI solution containing only tide station data is labeled as "T-obs" and the Foreman tidal model result is labeled as "F".

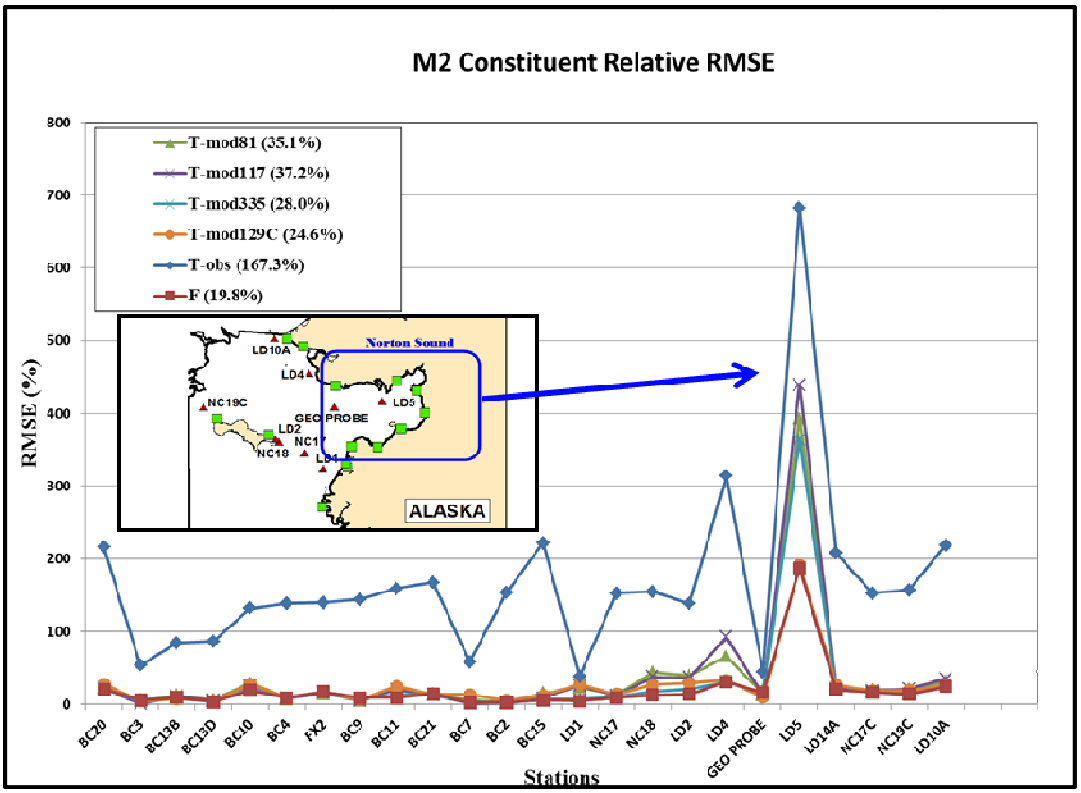

Figure 9. Relative RMSE values of the M2 constituent for the six comparison scenarios at each of the PMEL locations. Highlighted is the spike at the LD5 location and a subset map showing the location of LD5 within Norton Sound. The averaged relative RMSE values for each scenario are listed beside each label in the legend.

As indicated in Figure 9, the average relative RMSE value for the T-obs solution is 167%. This highlights a limitation of using TCARI for offshore extrapolation using only onshore observation data. The Foreman tide model, itself, provides the lowest average error (19.8%) and seems to match the PMEL data at all but the LD5 location. The results from the blended solutions using evenly distributed points improve with a higher data density, but the clustered solution has the lowest average error of all the blended scenarios. Overall the blended solutions result in significantly (nearly an 80% decrease in relative RMSE from the T-obs) lower M2 relative RMSE values. The reason why the Foreman tide model has the lowest average RMSE is that all of the 24 PMEL stations are offshore and the Foreman model performs well offshore by assimilating satellite altimetry data.

The highest averaged M2 errors of the six scenarios occurred at the location of the LD5 PMEL gauge. It is not surprising that the region with the largest relative errors for the M2 constituent is Norton Sound, since the amplitude of the M2 constituent is small in the diurnally-dominated sound. The observed amplitude of the M2 constituent at the LD5 PMEL gauge is only 0.02m; any measurable deviation from this number results in a large relative RMSE.

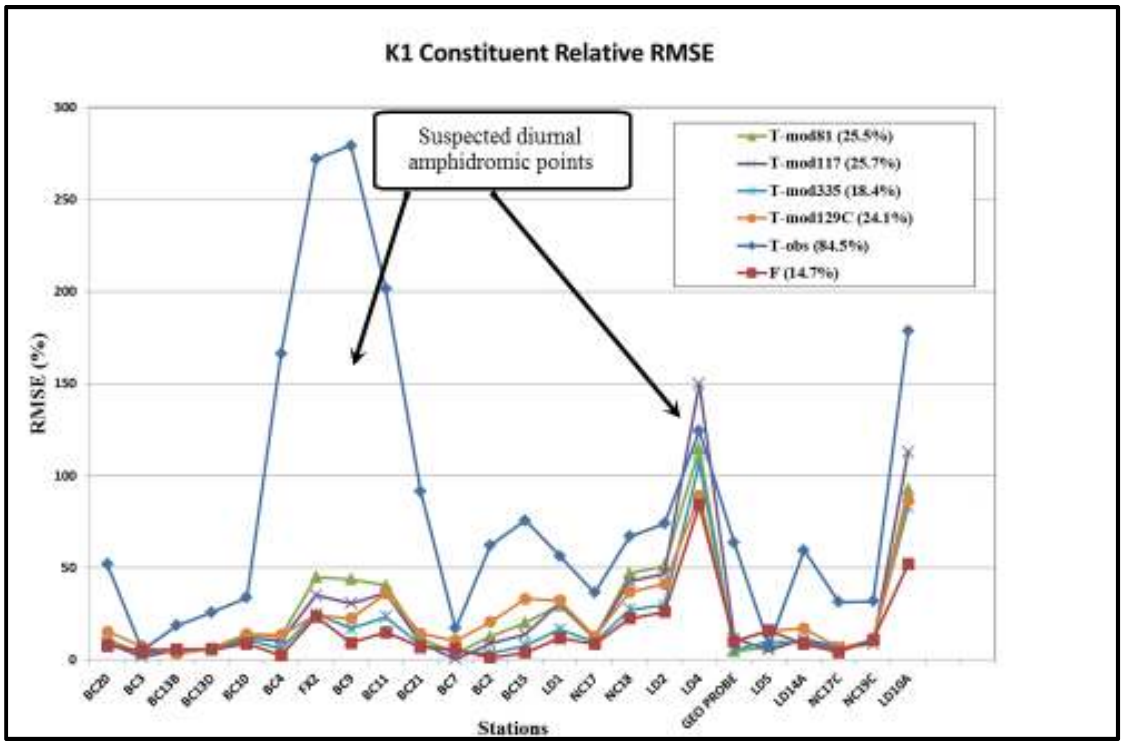

Figure 10. Relative RMSE values for the K1 constituent for the six comparison scenarios at each of the PMEL locations. Highlighted are the spikes at suspected amphidromes. The averaged relative RMSE values for each scenario are listed beside each label in the legend.

The relative RMSE values for K1 are shown in Figure 10 and highlight large discrepancies at two locations of modeled diurnal amphidromic points. The large T-obs errors located in the vicinity of BC4, FX2, BC9, BC11, and BC21 suggest that the interpolation of HCs derived from coastal observations cannot adequately represent the complex hydrodynamic environment in the vicinity of these PMEL gauges. This location is also a suspected diurnal amphidromic point (see Figure 11) and it is not surprising that an interpolated scheme, based entirely upon coastal data, cannot adequately capture a complex, offshore hydrodynamic feature. All of the six scenarios have consistently higher errors at LD4, which is in the vicinity of another suspected diurnal amphidromic point (see Figure 11). Additionally there is a large error at the LD10A location. One possible reason for the higher errors here is that the diurnal amplitude is only ~4cm; thus any error relative to this amplitude will be large. Overall the blended solutions provide a more accurate representation of the diurnal tide than the solution based entirely upon the interpolation of coastal HCs.

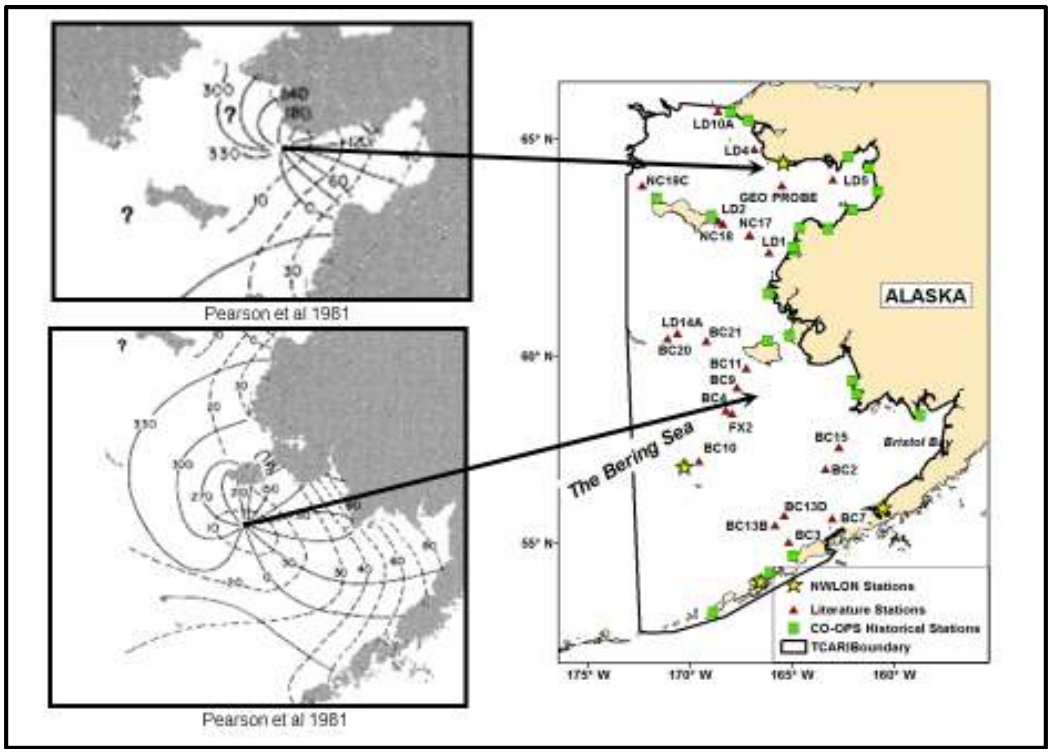

Figure 11. Relative positions of two diurnal (K1) amphidromic points outlined in the Pearson et al 1981 paper and the locations of the PMEL gauges used in the evaluation.

Phase contours of the M2 constituent from the six scenarios are show in Figure 12. It is interesting to note that the T+obs plot does not reveal any single semidiurnal amphidromic point, while the other five solutions, including the tide model-only solution, show both full and semi-amphidromic semidiurnal points off of the southwestern tip of the Seward Peninsula, inside of Norton Sound, off of the southeastern end of St Lawrence Island, and in Bristol Bay. The T+129 clustered result identifies the same semidiurnal amphidromic points as the Foreman tide model does but has the added operational benefit of including coastal observations. The result of the T+335 evenly distributed solution is similar to the clustered solution, but the significant increase in the number of points might present an operational limitation. The T+81 and T+117 evenly distributed solutions do not resolve all of the suspected amphidromes that the Foreman tide model shows.

Plots of the K1 phases in Figure 13 below suggest that the clustered solution most adequately reproduces the two suspected diurnal amphidromic points. The T+obs solution resolves a full amphidromic point off of the southwestern tip of the Seward Peninsula, which is consistent with Pearson (1981) (see Figure 11), while the model only identifies it as a semi-amphidromic point. The T+obs solution does not capture the changes associated with the amphidrome in western Bristol Bay while all four blended solutions show an amphidromic point similar to that found in the Foreman tide model.

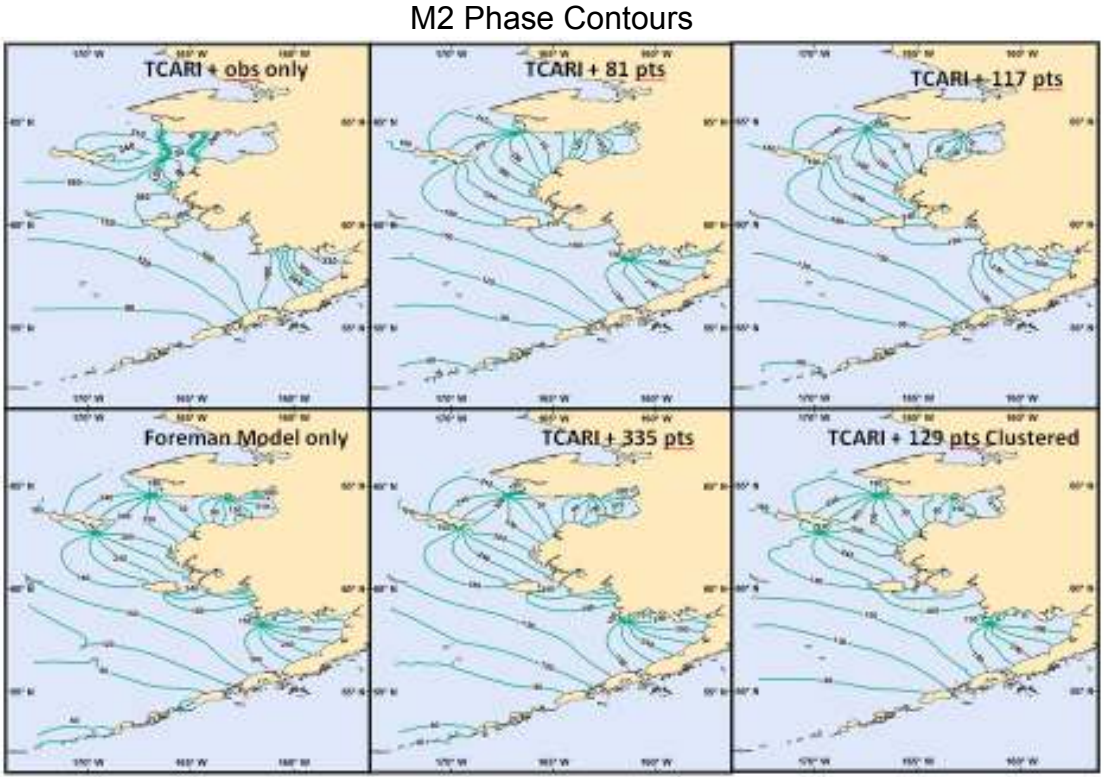

Figure 12. Phase contours of the M2 constituent generated from each of the six scenarios.

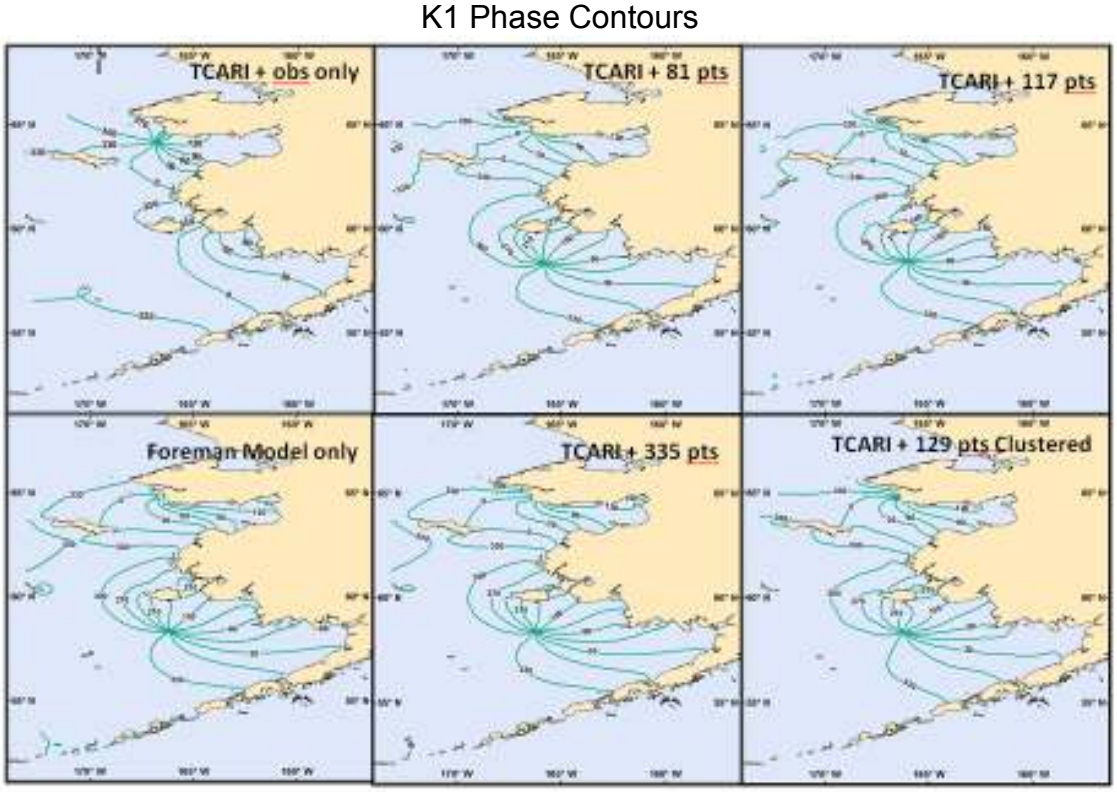

Figure 13. Phase contours of the K1 constituent generated from each of the six scenarios.

4. Discussion and Future work

The comparison of relative RMSE values and phase contours of the 6 scenarios indicates that the inclusion of model output into TCARI improves the interpolation results. Although there are some areas of significantly high relative RMSE values, such as LD4 and LD5, the values at these locations are still reduced as compared to the T+obs scenario. Additionally, the inclusion of model output significantly reduces the error in the vicinity of amphidromic points. These results indicate that the inclusion of model output into TCARI tide reduction schemes should be considered in areas of complex tidal hydrodynamics or in areas which lack a sufficient number of observations.

Given the same number of model points, the clustered method of selecting model points shows less relative RMSE when compared to the evenly distributed methods of selection (Figure 9, 10, 12 and 13). However, the evenly distributed method of selecting points is operationally more efficient and objective.

An additional sensitivity test was performed using the evenly distributed method of selection. The goal was to test the sensitivity of the spatial density parameter by setting it to 6 different values: 400km, 300 km, 200km, 100km, 50km, and 20km. Additionally, the buffer parameter was set to equal half of the spatial density parameter and the distance-away-from-station parameter was fixed at 50km. The results of this sensitivity test are shown in Figure 14. The average error reduces significantly when model output spaced at 400km is included in the TCARI solution. This improvement in RMSE is less dramatic when reducing the density parameter further. The trend is the same for both the M2 and K1 constituents. These types of sensitivity tests are important in order to maximize results while minimizing computer processing time. For the Bering Sea, the use of model output at the 400km grid level provides a sufficiently low error to support hydrographic surveys conducted by NOAA (NOS,2014).

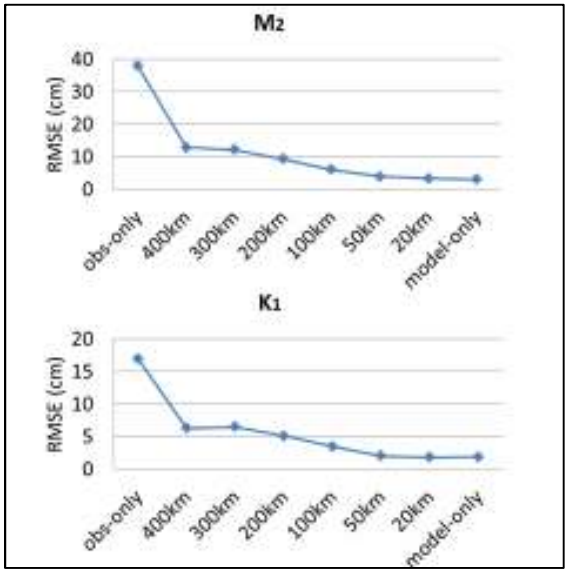

Figure 14. Model output inclusion sensitivity test with difference spatial densities but the same searching buffer parameter and the distance-away-from-station parameters. The RMSE is calculated using Equation 1.

Future testing of the results of TCARI solutions incorporating model points will be performed in regions of well-understood tidal physics using output from well-researched tidal models such as San Francisco Bay and Chesapeake Bay. Both San Francisco Bay and Chesapeake Bay are well bounded by both active and historical CO-OPS water level stations and this abundance of data creates an ideal environment for sensitivity tests. Both of the bays are much smaller than the Bering Sea, do not have the diversity of tidal regimes that are present in Bering Sea, and do not have an open boundary with limited offshore observations. Additionally, San Francisco Bay and Chesapeake Bay are the domains of two high resolution VDatum models (Yang et al. 2008, Xu et al. 2010). The output of the VDatum models will be used to enhance TCARI's interpolation within the bays and potentially improve TCARI solutions.

Evaluating the performance of TCARI supplemented with model output in San Francisco Bay and Chesapeake Bay will allow for the concept of blending model points and observations to be validated for future operational use by CO-OPS. Additionally, the results from the sensitivity tests in San Francisco Bay and Chesapeake Bay will be used to establish operational guidance on the selection and integration of model points.

Conclusion

Initial testing of integrating hydrodynamic model output with onshore observations to support the development of TCARI grids in the Bering Sea was performed and evaluated. The results indicate that the addition of model output into a TCARI solution reduced the relative RMSE of the interpolated M2 tidal constituent by nearly 80% and the K1 tidal constituent by nearly 70%. The method will be further tested in regions of well-understood tidal hydrodynamics and the domains of existing high resolution VDatum models, specifically, the San Francisco Bay and Chesapeake Bay areas.

References

Foreman, M.G.G.; Cummins, P.F.; Cherniawsky, J.Y.; Stabeno, P., Tidal energy in the Bering Sea. *J. Mar. Res.* 2006, 64, 797-818.

Hess, K.W., Spatial interpolation of tidal data in irregularly-shaped coastal regions by numerical solution of Laplace's equation. *Estuar. Coast. Shelf Sci*. 2002, *54*, 175-192.

Hess, K.W., Water level simulation in bays by spatial interpolation of tidal constituents, residual water levels, and datums. *Cont. Shelf Res*. 2003, *23*, 395-414.

Kowalik, Z., 1999. Bering Sea Tides. In *The Bering Sea: Physical, Chemical and Biological Dynamics*, Loughlin, T.R., Ohtani, K.O. (eds.), Alaska Sea Grant Press, Fairbanks, AK, pp. 93–127.

Liu, S.K. and Leendertse, J.J., Three-dimensional Model of Bering and Chukchi Sea. *Coastal Engineering*, 1982, 18:598-616.

Mofjeld, H.O., Observed Tides on the Northeastern Bering Sea Shelf. *J. Geophys. Res*., 1986, 91:2593-2606.

NOS, 2014. NOS Hydrographic Surveys Specifications and Deliverables, 2014 Edition, NOAA/NOS Office of Coast Survey, (available at: http://www.nauticalcharts.noaa.gov/hsd/specs/specs.htm)

Pearson, C.A., Mofjeld, H. O. and Tripp, R. B., 1981. Tides of the Eastern Bering Sea Shelf. In *The Eastern Bering Sea Shelf: Oceanography and Resources*, Hood, D and Calder, J. A. Calder (eds), Vol. 1, USDCS/NOAA/OMPA, pp. 111-130.

Xu, J., E. Myers, S. White (2010). VDatum for the Coastal Waters of North/Central California, Oregon and Western Washington: Tidal Datums and Sea Surface Topography. NOAA Technical Memorandum NOS CS 22.

Yang, Z., E. Myers, A. Wong, S. White (2008). VDatum for Chesapeake Bay, Delaware Bay and adjacent coastal water areas: Tidal datums and sea surface topography. NOAA Technical Report NOS.

Author Biographies

Lijuan Huang has worked for NOAA/NOS/CO-OPS as an oceanographer since 2006. She holds a M.S. in Geological Oceanography from the Marine Science Research Center of Stony Brook University School, NY and a B.S. in Physical Oceanography from Xiamen University in China.